Indian Journal of Biochemistry & Biophysics
Vol. 63, July 2026, pp. 810-822
DOI: 10.56042/ijbb.v63i7.18129

Development and bioevaluation of chitosan hydrogels infused with chondroitin sulphate and ferulic acid for wound healing

Marwan Salem Bahaj[1], Marwan Abdelmahmoud Abdelkarim Maki[1]*, Palanirajan Vijayaraj Kumar[1], Sasikala Chinnappan[1], Mogana Rajagopal[1], Tan Kin Fai[1] & KRS Sambasiva Rao[2]

[1]Faculty of Pharmaceutical Sciences, UCSI University, Kuala Lumpur-56000, Malaysia

[2]School of Pharmacy, Dr. RVR NRI Institute of Technology Deemed to be University, Pothavarappadu (V), Agiripalli Mandal, Vijayawada Rural-521 212, Andhra Pradesh, India

Received 21 July 2025; *revised 18 March 2026*

Chitosan hydrogels are recognized as promising wound dressings as they can mimic extracellular matrix, retain moisture and deliver therapeutic agents. In this study, chitosan hydrogel enriched with chondroitin sulphate (CS) and ferulic acid (FA) is prepared to improve wound healing and antibacterial effects. The characterization studies were conducted to measure the hydrogel mechanical strength, swelling capacity, moisture retention and polymer-therapeutic agents compatibility. *In vitro* release studies were conducted and a revealed sustained CS release of 98.95% within 48 h, while FA shown limited diffusion of 3.48%. Antibacterial properties of the prepared hydrogel was tested against Staphylococcus aureus and revealed 15.0 mm ±0.8 mm inhibition zone (n = 3), suggesting antibacterial effect. The ability of the prepared hydrogel to improve fibroblast cells migration and wound closure was measured using scratch assay. Moreover, the potential interactions between the bioactive compounds and proteins associated with wound healing pathways was measured using molecular docking. The combination of CS and FA within the chitosan hydrogel suggested a promising strategy for enhancing tissue regeneration, wound management and public health.

Keywords: Controlled release, Fibroblast migration, Matrix metalloproteinase modulation, Polymer-drug interaction

Skin is the largest organ of the body and serves as the primary barrier against microbial invasion, environmental exposure, and physical injury[1]. Wound healing occurs in a series of biological events that can be broken down into haemostasis, inflammation, proliferation, and tissue remodelling[2]. In chronic wounds like diabetic ulcers, burns and pressure sores, the major healthcare problem is delayed or impaired healing which may lead to infection, excessive scar formation, and in severe cases amputation[3]. In developing countries, chronic wounds affect 1 to 2% of the population, and diabetic foot ulcers affect nearly 25% of the global diabetic population[4,5]. The high prevalence of chronic wounds also represents a high economic burden for wound treatment and management, with the global wound care market predicted to reach USD 29.6 billion by 2026[6].

Ideally, a wound dressing should maintain moisture at the wound site, allow for gas exchange, minimize microbial contamination, promote cell growth, and deliver therapeutic agents in a controlled manner[7,8]. Hydrogels have been extensively studied in wound management due to their high water content, biocompatibility, and ability to mimic ECM structures involved in tissue repair[9]. They can also absorb wound exudates, maintain hydration, and serve as a physical barrier to external contaminants[10]. However, the addition of appropriate bioactive compounds remains essential for their enhanced therapeutic efficiency.

Chitosan (CHI) is one of the most researched natural polymers for wound healing applications due to its biodegradability, antimicrobial activity, haemostatic properties, and ability to stimulate fibroblast proliferation[11]. For instance, previous reports indicated that CHI-based wound dressings may reduce healing time by as much as 30% compared to traditional wound dressings[12]. Chondroitin sulphate (CS), another glycosaminoglycan naturally found in connective tissues, has also been incorporated into hydrogel systems as it is capable of promoting extracellular matrix remodelling, modulating cellular interactions, and enhancing the mechanical properties of the material[13]. Preliminary studies showed that CS-based biomaterials enhanced wound healing rates by up to 40% in preclinical studies[14].

*Correspondence:
E-mail: marwanaamaki@gmail.com

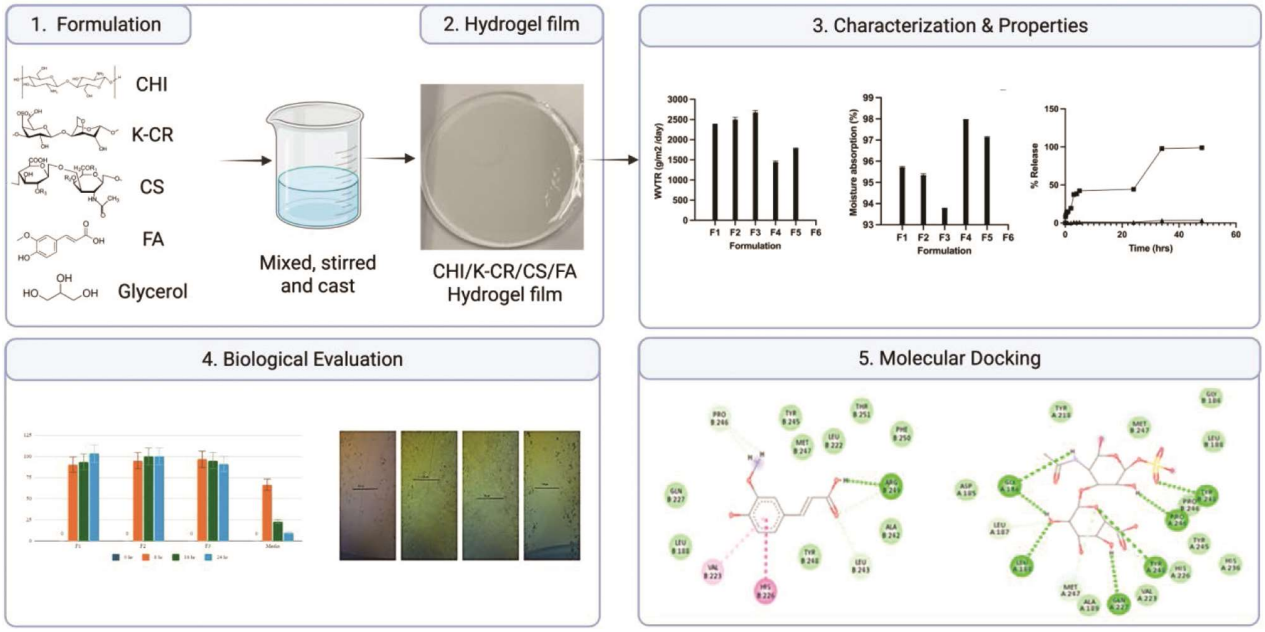

Graphical abstract

Another compound of interest in wound healing formulations is ferulic acid (FA), which possesses antioxidant, anti-inflammatory, and antimicrobial properties[15]. FA has been previously reported to reduce oxidative stress markers by nearly 50% and decreased bacterial growth by approximately 60%[16], scavenge ROS, inhibit lipid peroxidation, and inhibit the release of pro-inflammatory cytokines[17], which all may enhance wound healing responses.

Both CS and FA are typically combined into topical formulations, as they offer complementary biological activities, and CS concentrations are typically 0.1% to 1.0% and FA concentrations are typically 0.01% to 0.1% in most formulations, with 0.3% CS and 0.05% FA chosen in the present work to achieve suitable stability, solubility, and biocompatibility with retained therapeutic effects. The developed hydrogel combines CHI for antimicrobial and regenerative functions, CS for extracellular matrix-related support, and FA for antioxidant and anti-inflammatory activities. Considering the increasing prevalence of chronic wounds, development of improved biomaterials for wound treatment remains important. Therefore, this study was conducted to prepare and characterize chitosan-based hydrogels enriched with CS and FA and to evaluate their physical, chemical, and biological properties in relation to wound healing and antibacterial activity.

Materials and Methods

Reagents and cell Culture

Chitosan (Sigma-Aldrich, Germany), Chondroitin sulphate (Sigma-Aldrich, Germany), Carrageenan (Sigma-Aldrich), Ferulic acid (Merck, Germany), Phosphate-buffered saline (PBS) (Hampshire, England), Glycerol (Zulat pharmacy SDN BHD, Malaysia), Sartolon polyamide filter (Gottingen, Germany), Mueller Hinton Agar (Madrid, Spain), Nutrient broth (Merck, Germany), MRC-5 - CCL-171 (ATCC, USA), Fetal Bovine Serum (FBS) (Gibco, USA), streptomycin/penicillin solution (Gibco, USA), trypsin/EDTA (Gibco, USA), Eagle's Minimum Essential Medium (EMEM) (ATCC, USA).

Preparation of CHI /κ-CR/CS/FA Hydrogel Film

Hydrogel films were prepared using two separate solutions. First, 1% kappa-carrageenan (κ-CR) was dissolved in 30 mL distilled water and heated at 50°C for 20 min or until completely dissolved. Another solution containing 1% CHI, 0.7% CS, and 0.033% FA was prepared in a separate beaker and stirred continuously at 50°C for 10 min to obtain a uniform mixture. After that, the two solutions were mixed together and glycerol was then added in 0.83% concentration as a plasticizer. The mixture was then stirred for 15 min to obtain complete homogenization[18]. The prepared hydrogel solution was poured into petri dishes and dried in an oven at 50°C for 24 h to produce solid hydrogel films (Fig. 1).

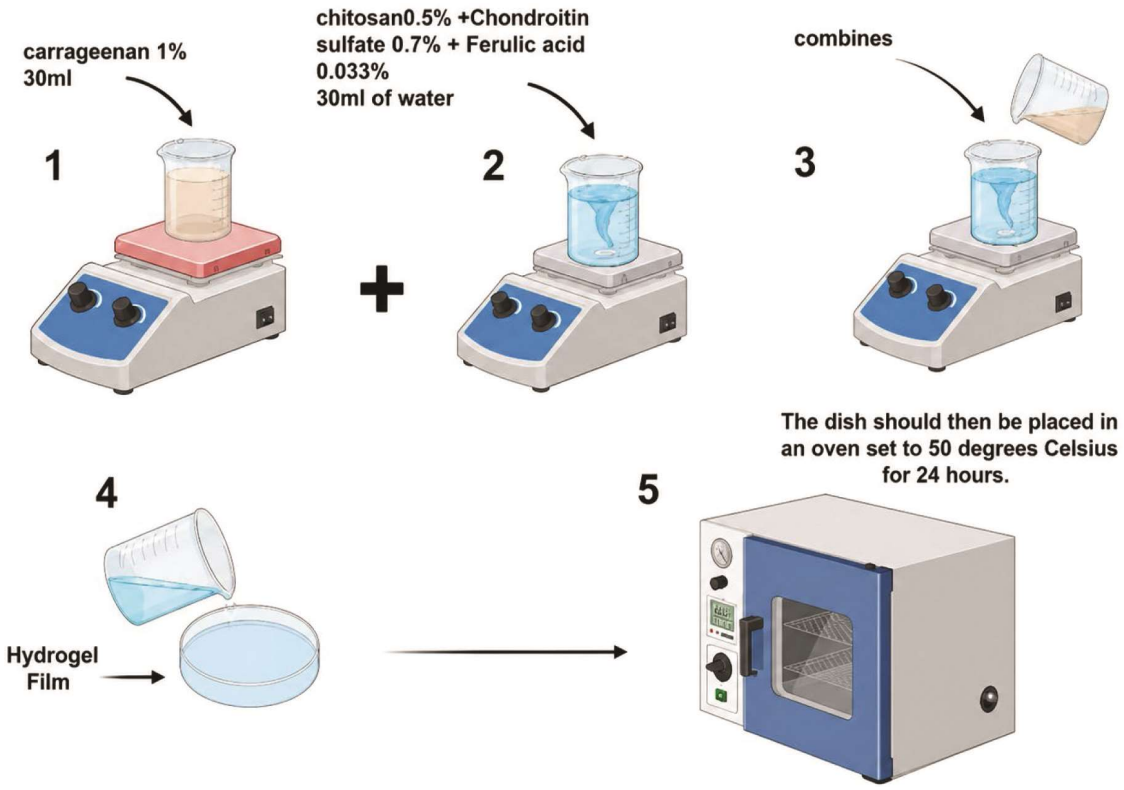

Fig. 1 — Preparation of κ-CR/ CHI /CS/FA hydrogel film

Table 1 — Since different batches of hydrogel films are going to be prepared, a composition table is prepared below

Formulation	CHI	κ-CR	CS	FA	Glycerol
F1	0.5%	1%	0.7%	0.1%	0.83%
F2	0.75%	1%	0.7%	0.066%	0.83%
F3	1%	1%	0.7%	0.033%	0.83%
F4	1%	0.5%	0.7%	0.016%	0.83%
F5	1%	0.75%	0.7%	0.01%	0.83%

Different concentrations of CHI, κ-CR, CS, and FA were evaluated during the formulation optimization studies to investigate their effects on swelling behaviour, mechanical properties, water vapor transmission rate, and moisture retention capability (Table 1).

Film Thickness

Film thickness was measured at five randomly selected positions on the hydrogel film using a digital micrometer. Mean thickness values and their standard deviations were calculated and reported[19].

Swelling Ratio

Dried hydrogel films were cut into 2 cm × 2 cm squares and placed in 250 mL of phosphate-buffered saline (PBS, pH 7.4) at 25°C and removed at predetermined time intervals. Surface moisture was blotted with tissue paper, and the swollen films were weighed. The swelling ratio was calculated as follows:

$$\text{Swelling ratio (\%)} = \frac{W_s - W_d}{W_d} x\ 100$$

where Wd is the initial weight of dry film samples and Ws is the weight of swollen film samples[20].

Mechanical Properties

The tensile strength (TS) and percentage elongation (%E) at break were measured using a texture analyzer (electrodynamic fatigue testing machine, 1.5 KN). Dumbbell-shaped hydrogel membranes were placed between clamps, stretched at a rate of 5 mm/min until rupture. TS and %E were calculated using[21].

$$\text{Ts} = \frac{maximum\ load\ at\ break}{transverse\ section\ area}$$

$$\%E = \frac{Extension\ of\ length\ at\ rupture}{initial\ length}\ X\ 100$$

Water Vapor Transmission Rate

Water vapor transmission rate (WVTR) was measured using the bottle method. Cylindrical bottles filled with 10 mL distilled water were sealed with hydrogel membrane discs and secured using Teflon tape. The bottles were placed in an oven at 35°C for 24 h[22]. WVTR was calculated by:

$$\text{WVTR} = \frac{Wi - Wt}{A\ X\ 24}\ X\ 10^6 gm^{-2}h^{-1}$$

Moisture Retention Capability

Moisture retention capability was assessed by weighing hydrogel samples, then drying them at 40°C for 6 h and reweighing[23]. The percentage moisture retention was calculated using:

$$\text{Moisture retention capability } (\%) = wt/(wi\ x\ 100)$$

Fourier Transform Infrared Spectroscopy

FTIR spectra of dried hydrogel films (100-200 µm thickness) were recorded using an FTIR-8400S spectrometer (Shimadzu Europe) from 450 to 4000 cm^{-1}. Spectra were normalized, and characteristic vibration bands were identified[24, 25].

***In vitro* Drug Release Study**

The *in vitro* release of CS from hydrogel films was studied using Franz diffusion cells with PBS (pH 7.4, 37°C). At specific time intervals, samples were collected, replaced with fresh PBS, and analysed by UV spectroscopy at 260 nm[26]. Drug release data were fitted to: Zero-Order ($Q_t = k_0 t$, constant release), First-Order [$Q_t = 100\left(1 - e^{-k_t t}\right)$, concentration-dependent], Higuchi ($Q_t = k_H\sqrt{t}$, diffusion-controlled), and Korsmeyer-Peppas ($Q_t = k_p t^n$, polymer interaction-based)[27–29]. The R^2 values were calculated to identify the best-fitting model for CS and FA release behavior.

Antibacterial Tests

To determine the antibacterial activity of CHI-based hydrogels containing CS, a well diffusion method was employed, with Mueller-Hinton Agar medium for bacterial growth and freshly grown overnight cultures of gram-positive bacteria (*S. aureus*) adjusted to 1×10^3 CFU/mL using turbidity measurements and plated with 100 µL of suspension in 16 mL of solidified nutrient agar plates using a sterile agar punch to create wells of approximately 6 mm diameter. The wells were spaced such that diffusion zones did not overlap between wells to avoid overlapping inhibition zones, and the hydrogels were loaded into the wells using a sterile pipette and a volume sufficient to fill each well completely. The CHI-based hydrogels enriched with CS at the highest concentration and control were tested for their antibacterial activity at different concentrations of the drug. The plates were incubated at 37°C for 24 h to allow for diffusion of the hydrogel components into the agar and subsequent growth inhibition[30].

Molecular Docking

AutoDock Vina-Extended SAMSON (version 4.0.3) was used to perform molecular docking, using the interactions of the native ligands as a binding site for 4H1Q and 5A0C, which were cleaned and optimized, and all ligands were minimized (Et = 0.025 kcal/mol). The water molecules were removed, and the flexible docking was performed to generate 10 poses for each docking session. The highest ranked pose for each ligand was visualized and analyzed for protein-ligand interactions, including hydrogen bonding and non-covalent interactions, using the Ligand-Protein Interaction Analyzer extension in SAMSON[31].

Scratch Assay

MRC-5 cells were plated in triplicate in a 24-well plate and incubated at 37°C under a humidified atmosphere with 5% CO2 and 95% air to achieve a confluent monolayer; uniform scratches were made in the cell monolayer using a p-10 pipette tip and the cells were followed for 24 h as they filled in the scratched area; images were captured using a light microscope (Axio Vert.A1, Carl Zeiss, Germany), and wound healing was quantified by measuring the distance between the migrating cell boundaries using ImageJ 1.47 software (National Institutes of Health, Bethesda, MD, USA). Wound healing was reported as a relative percentage change in the distance between the migrating cell boundaries from the beginning to the end of each treatment[32-36].

Statistical Analysis

All experiments were repeated in triplicate unless otherwise indicated, and data are presented as mean ± standard deviation (SD). Statistical analysis was conducted using SPSS V27, and comparisons between groups were made using one-way analysis of variance (ANOVA) followed by Tukey's post hoc test. Statistical significance was set at $P < 0.05$.

Results and Discussion

Film Thickness

Hydrogel film thickness depends on factors such as the polymer concentration, preparation method, casting volume, and drying conditions. To minimize thickness variations in this study, an equal quantity (25 g) of hydrogel solution was carefully cast into each petri dish. The resulting hydrogel films showed an average thickness ranging from 0.092 mm (F3) to 0.118 mm (F1) (Fig. 2 & Table 2).

Swelling Ratio

To determine the suitability of the prepared hydrogel films for wound healing applications, their swelling ratio (SR) was measured *in vitro*. All prepared formulations (F1 to F5) which contained different concentrations of CHI, κ-CR, CS, FA and glycerol have shown SR values from 106.91% (F1) to 225.39% (F5) (Fig. 3). F5 exhibited the highest SR of 225.39%, suggesting its capability for exudate absorption in chronic wounds management. The high SR value can be related to the lower concentration of κ-CR incorporated in F5, reducing the rigidity of film matrix and increase fluid uptake capability. Studies have suggested that higher SR values are preferred for wound dressings to maintain a moist environment to promote cellular proliferation and angiogenesis[37].

Fig. 2 — CHI/κ-CR/CS/FA hydrogel film

Mechanical Properties

Ideal wound dressings should exhibit suitable mechanical properties, including tensile strength (TS) and elongation at break (%E), to mimic skin integrity and flexibility. Typically, natural skin shows a tensile strength ranging from 2.5 to 35 N and elongation at break between 70 to 78%. In this study, the prepared hydrogel films exhibited tensile strength values ranging from 8.36 ± 0.43 N (F4) to 11.06 ± 0.17 N (F3). These results indicate that the hydrogel films possess adequate strength to maintain structural integrity and sufficient flexibility to withstand natural deformation when applied as wound dressings. These findings are in line with those previously reported for classical chitosan-based hydrogels for wound healing (5 to 10 N [0.5 to 1.0 MPa] depending on formulation details[38]) that are likely due to the enhancement of polymer cross-linking and matrix integrity by the inclusion of chondroitin sulphate and ferulic acid. Additionally, elongation at break values ranging from 41.58 ± 0.22% (F4) to 46.00 ± 0.92% (F3) (Table 2) demonstrate that the hydrogel membranes are flexible enough to follow irregular wound geometries without breaking, a requirement for dressing flexibility during patient movement.

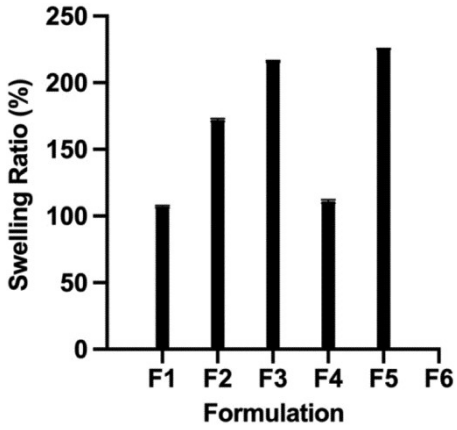

Fig. 3 — Swelling ratios of the prepared hydrogel films

Table 2 — Thickness, swelling ratio, tensile strength, and elongation at break (%) parameters for batches of hydrogel films (n = 5)

Formulation code	Thickness (mm)	Tensile Strength (N)	Elongation at Break (%)
F1	0.118 ±0.020	10.30 ± 0.29	45.67 ± 0.24
F2	0.101 ±0.009	10.25 ± 0.40	44.24 ± 0.20
F3	0.092 ±0.045	11.06 ± 0.17	46 ± 0.92
F4	0.116 ±0.007	8.36 ± 0.43	41.58 ± 0.22
F5	0.096 ±0.050	10.60 ± 0.05	45.08 ± 0.66

Water Vapor Transmission Rate

Hydrogel films are useful for managing moisture levels at the wound site, and the WVTR is an important parameter. For example, in formulations F1 to F3, increasing the concentration of CHI from 0.5% to 1% (while κ-CR was held constant at 1%) increased the WVTR, indicating that higher CHI levels increased film permeability. In contrast, formulations F4 and F5, which had constant CHI (1%) but with varying κ-CR concentrations, showed that lowering κ-CR to 0.5% (F4) had a significant decrease in WVTR, whereas a moderate increase to 0.75% κ-CR (F5) increased WVTR but less than formulations F1 to F3.

Moisture Retention Capability

Moisture retention is important for the wound healing process because moisture loss decreases the temperature of the wound bed, increases metabolic rate, and impairs healing. In general, the WVTR is inversely related to the moisture retention capability of hydrogel membranes, and formulations F4 and F5, with lower WVTR, showed better moisture retention (Fig. 4a & b); formulations F1, F2, and F3, with higher concentrations of hydrophilic κ-CR, had higher WVTR, leading to reduced moisture retention capability. These results suggest that the hydrophilic polymer content needs to be carefully balanced to provide the optimal moisture environment for wound management.

Fourier Transform Infrared Spectroscopy

As seen in the FTIR spectra of the κ-CR, CHI, CS, FA, and glycerol hydrogel films (Fig. 5), significant molecular interactions between the formulation components were observed. A wide peak around 3292.05 cm^{-1} suggests extensive hydrogen bonding,

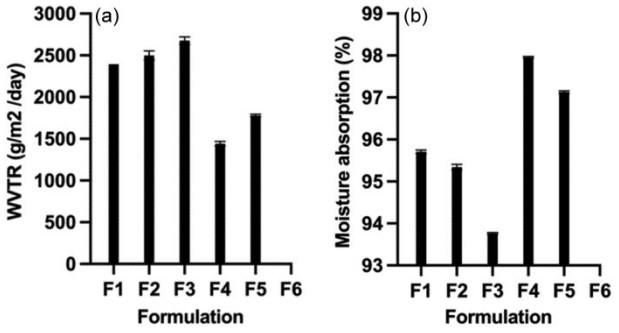

Fig. 4 — WVTR (A) and % moisture absorbance (B) from κ-CR/CHI/CS/FA Hydrogel Film

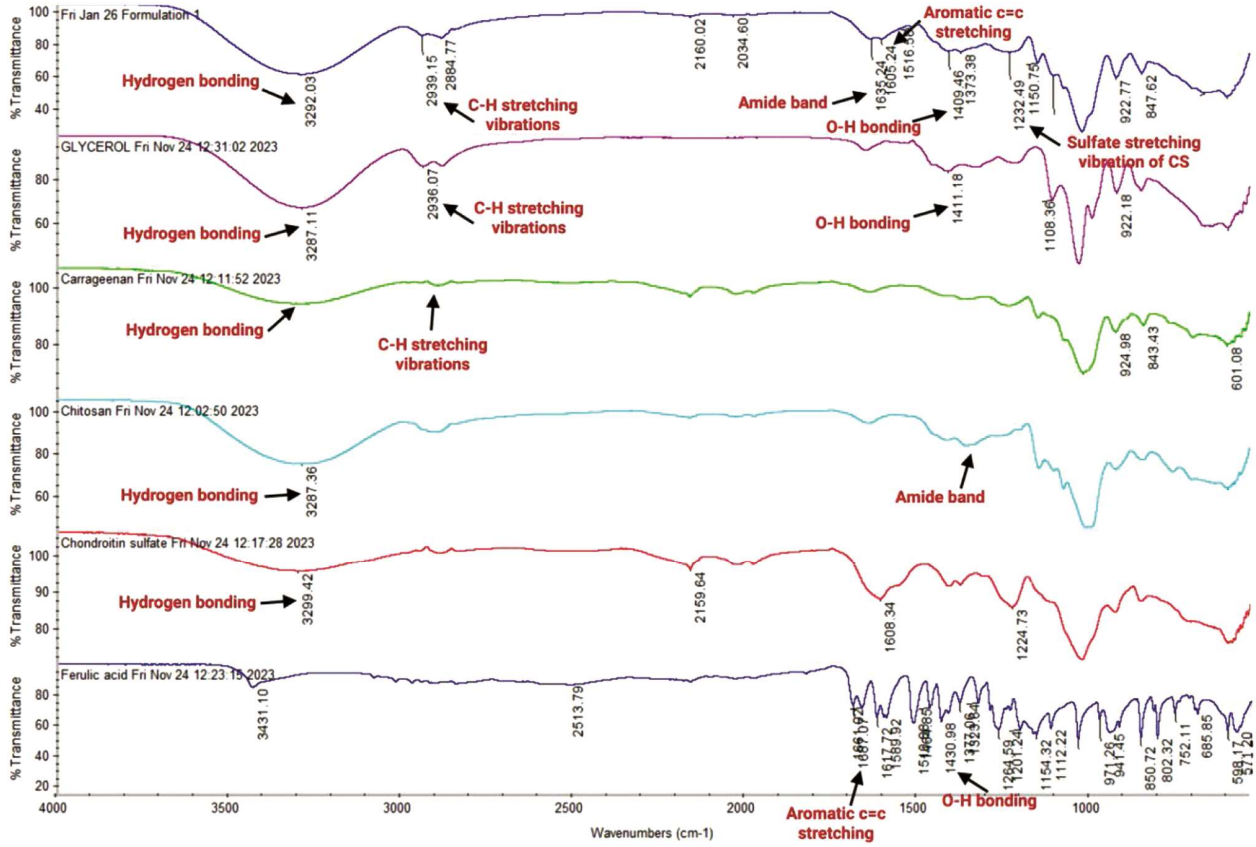

Fig. 5 — FTIR spectra of κ-CR, CHI, CS, FA, and glycerol hydrogel films

perhaps between hydroxyl groups of the hydrogel constituents. The shifts in CH stretching vibrations at 2939.15 cm^{-1} and 2849.17 cm^{-1} (methylene and methyl groups) are consistent with their different molecular environments arising from the proximity of the components. For instance, the amide peak of CHI shifted from 1654.55 cm^{-1} to 1648.07 cm^{-1} and the carbonyl peak of FA shifted slightly from 1733.86 cm^{-1} to 1731.83 cm^{-1}, both consistent with hydrogen-bonded interactions. Furthermore, the sulphate vibration of CS moved from 1224.73 cm^{-1} to 1222.26 cm^{-1}, indicating ionic interactions between the negatively charged sulphate groups of CS and positively charged amine groups of CHI. The fingerprint region (below 1500 cm^{-1}) also displays overlapping peaks, which reflects complex molecular interactions that contribute to structural integrity, swelling behaviour, mechanical stability, and controlled drug release, suggesting successful integration within the hydrogel matrix.

In vitro Drug Release Study

CS exhibited a steady, gradual release profile from the hydrogel, with an initial release of 8.22% at 0.167 h and nearly complete release (98.95%) after 48 h (Fig. 6), which is consistent with a Korsmeyer-Peppas release pattern (R^2 = 0.967), indicating diffusion-driven release with possible polymer relaxation effects, and was confirmed by a high correlation with the Higuchi model (R^2 = 0.943) (Table 3). On the other hand, FA release was very low (initially negative, -0.14% at 0.167 h, probably because of initial absorption or adhesion), and only 3.48% after 48 h. The release of FA had a weaker relationship with the kinetic models, and the Korsmeyer-Peppas model (R^2 = 0.735) fit best, suggesting that there is significant polymer-drug interaction limiting diffusion. Even with this limited release, FA may still contribute to the overall therapeutic performance of the hydrogel; in topical wound dressing applications, complete release of bioactive compounds is not always necessary, since localized activity at the wound interface can be enough to elicit antioxidant and anti-inflammatory effects, and the retained FA within the hydrogel matrix may provide long-term local protection against oxidative stress and inflammation.

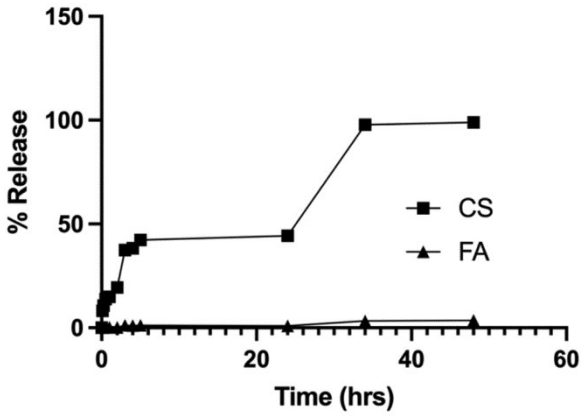

Fig. 6 — *In vitro* release profiles of CS and FA

Table 3 — R^2 values for kinetic model fitting of CS and FA release

Release kinetics model	CS, R^2 values	FA, R^2 values
Zero Order	0.872	0.615
First Order	0.925	0.678
Higuchi Model	0.943	0.702
Korsmeyer-Peppas	0.967	0.735

Antibacterial Tests

Hydrogel films containing 0.3% CS and 0.05% FA were evaluated for their antibacterial activity against S. aureus using the agar well diffusion method (n = 3), and results showed a clear inhibition zone with an average of 15.0 mm ±0.8 mm inhibition zone ($P<$ 0.05). These preliminary findings show that the hydrogel films containing CS and FA had a significant inhibitory effect against *S. aureus*, demonstrating the potential of the formulation as an antibacterial agent compared to previously reported CS/CHI-based hydrogels, which typically show zones in the range of 10-14 mm inhibition zone[39]. The synergistic antibacterial effect may result from the polycationic nature of the chitosan disrupting bacterial membranes, while FA contributes by inducing oxidative stress in microbial cells. While *S. aureus* is clinically relevant in wound infections, it does not fully represent the diverse microbial population found in infected wounds; thus, further studies will include a broader spectrum of wound-associated pathogens to more fully evaluate the antimicrobial performance of the formulation.

Protein-Ligand Docking and Interactions Analysis

The molecular docking study identified 4H1Q and 5A0C, two proteins directly involved in key biological processes related to wound healing and infection management. Protein 4H1Q (human matrix metalloproteinase-9, MMP-9) is involved in extracellular matrix remodelling, which is a vital step in wound repair and tissue regeneration. Protein 5A0C is related to inflammatory responses and is important in wound healing. The interaction of CS

and FA with these proteins can be assessed for their therapeutic potential in modulating wound healing pathways, as docking analyses for CS and FA showed multiple binding modes with different therapeutic implications (Table 4). For CS, strong interactions were observed with both proteins: The first binding mode with 4H1Q had high docking scores and minimal RMSD, a highly stable and precise interaction that will be necessary for effective therapeutic inhibition (Fig. 7c and Fig. 9a). The second mode had lower docking scores and higher RMSD values, which indicated alternative but therapeutically relevant binding conformations. Protein 5A0C showed similar trends, with the first mode having the best precision and stability (Fig. 7d and Fig. 9b), and the second mode having slightly lower affinity but still biologically relevant.

FA interactions with protein 4H1Q showed strong binding and high affinity and stability, with low RMSD in the primary mode (Fig. 7a and Fig. 8a), indicating energetically favorable interactions that are required for biological activity; the secondary mode showed higher RMSD values, indicating less stability, but still significant, showing that the compound is flexible in its conformation in the binding site. For protein 5A0C, the primary interaction mode was stable (Fig. 7b and Fig. 8b), whereas the secondary mode showed lower affinity but may still be of biological interest.

Table 4 — Summary of molecular docking outcomes conducted using AutoDock Vina software

S. No	Compound Name	PubChem CID	Protein PDB ID:4H1Q		Protein PDB ID:5A0C	
			Score	RMSD	Score	RMSD
1	FA	445858	-7.00	0.000	-5.90	0.000
2	FA	445858	-6.78	13.422	-5.80	10.398
1	CS	24766	-8.67	0.000	-7.50	0.000
2	CS	24766	-8.47	3.511	-7.47	1.665

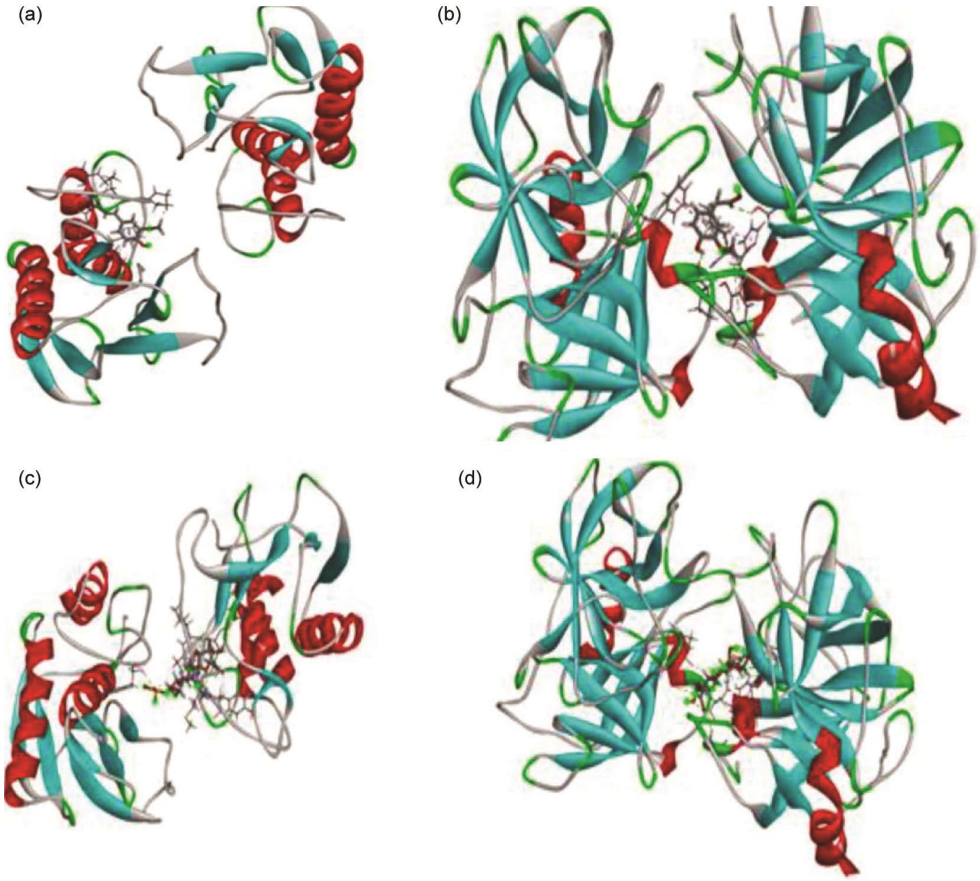

Fig. 7 — (a) FA interaction with 4H1Q; (b) FA interaction with 5A0C; (c) CS interaction with 4H1Q; and (d) CS interaction with 5A0C

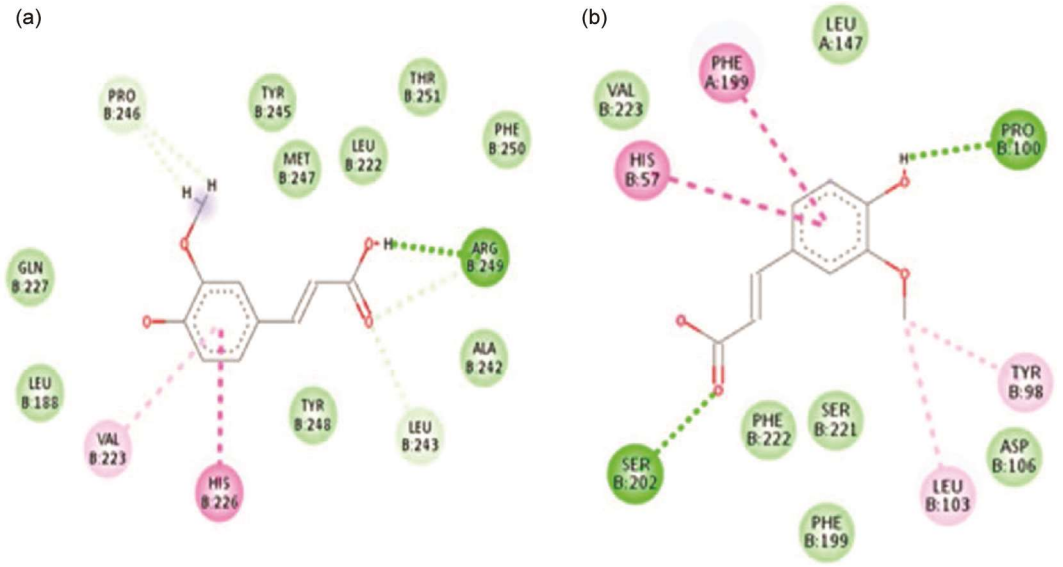

Fig. 8 — (a) Interaction map of FA with protein 4H1Q highlighting hydrogen bonds and hydrophobic interactions; and (b) detailed docking visualization of FA with protein 5A0C showing key molecular interactions

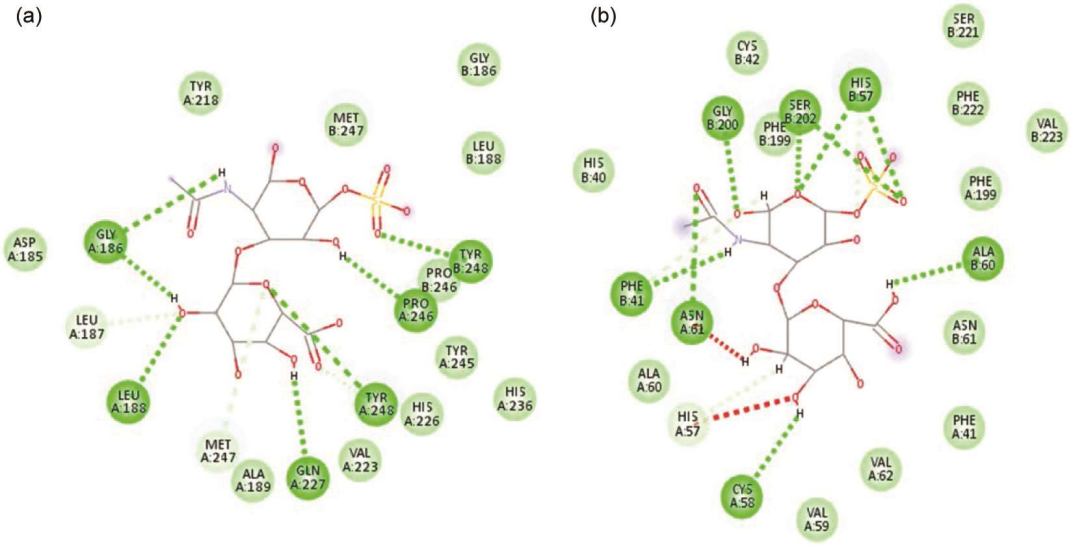

Fig. 9 — (a) Molecular interaction map of CS with protein 4H1Q highlighting key binding residues; and (b) detailed docking visualization of CS with protein 5A0C showing crucial molecular interactions

Hydrogen bonds and hydrophobic contacts were shown to be important in stabilizing ligand interactions in protein active sites. In FA, crucial hydrogen bonds with TYR B:245, ARG B:249, THR B:251 (protein 4H1Q), and PRO B:100, SER B:221 (protein 5A0C), and important hydrophobic interactions stabilized binding (Fig. 8). Also, CS interactions were stabilized by essential hydrogen bonds with GLY A:186, TYR B:246 (protein 4H1Q), ASN A:57, and SER B:202 (protein 5A0C) and were further strengthened by large hydrophobic interactions, indicating extremely optimized binding conformations (Fig. 9).

The range of RMSD values observed across different binding modes for both CS and FA can be attributed to the flexibility of the ligand, which can adopt a variety of conformations within protein binding sites, with lower RMSD values being indicative of high stability and biological relevance, while higher RMSD values may reflect alternative binding modes that are less energetically favorable but still could be pharmacologically active. This

information forms a solid basis for further structural optimization and therapeutic development of these bioactive compounds. The molecular docking analysis offers a preliminary computational prediction of potential interactions between the bioactive compounds and proteins associated with wound-healing pathways. CS showed a binding energy of -8.67 kcal/mol with MMP-9 (4H1Q), which indicates potential interaction with matrix metalloproteinase-related pathways that may be associated with wound healing, often elevated in chronic wounds, which can cause ECM degradation and delayed healing. Likewise, FA had favorable binding with pro-inflammatory mediators (5A0C), which suggests that it may modulate local inflammation at the wound site. The ability of the hydrogel system to stabilize ECM via CS and reduce inflammation via FA may account for this biological activity and warrants further exploration of the system. These preliminary computational insights require experimental validation, such as enzymatic inhibition assays, inflammatory marker analysis, or *in vivo* wound healing studies, to confirm the proposed mechanisms.

Scratch assay

The scratch assay showed increased fibroblast migration and *in vitro* wound closure for all formulations (F1, F2, and F3) tested over 24 h (n = 3), demonstrating their ability to promote cell migration and tissue regeneration. At 0 h, there was no significant difference in scratch widths between the groups, and at 8 h, a significant decrease in scratch width was observed for F1, F2, and F3 (early promotion of cell migration), with slower closure in the control group (media). At 16 h, formulations F1 and F2 were close to complete closure (>100%), with F3 also showing significant decrease (Fig. 10). At 24 h, formulations F1 and F2 reached closure percentages of 103% ±3% and 100% ±2%, respectively ($P< 0.05$). F3 (FA at 30 mg/mL alone) showed promise for use as a wound dressing (91% ±4%) but was less than polymeric combinations. The control group remained the slowest, with approximately 75% ±3% closure (Fig. 11). Cell migration increased significantly in the treated groups (F1, F2, and F3) compared to the control ($P< 0.05$), with the F1 group having the highest percentage of closure (103% ±3%) likely because of the glycerol-mediated hydration and increased cellular viability, whereas F2, which did not contain glycerol, achieved complete closure (100% ±2%), possibly due to the inherent effectiveness of the polymeric composition. These results demonstrate the potential of these hydrogels in wound management, and that F1 and F2 may have the best therapeutic outcomes.

These hydrogels exhibit combined mechanical, physicochemical, and bioactive properties, indicating great potential for clinical wound management, particularly in complex chronic wound environments, with added advantages of bioactivity (antibacterial and anti-inflammatory), sustained release, and ECM-mimetic behavior compared to commercial hydrogel dressings. Its translational potential for clinical applications may be further elucidated through further *in vivo* validation.

A few chitosan-based hydrogels containing natural bioactive agents like honey, garlic extract, and ferulic acid have been reported for wound healing applications, but most of them depend on a single

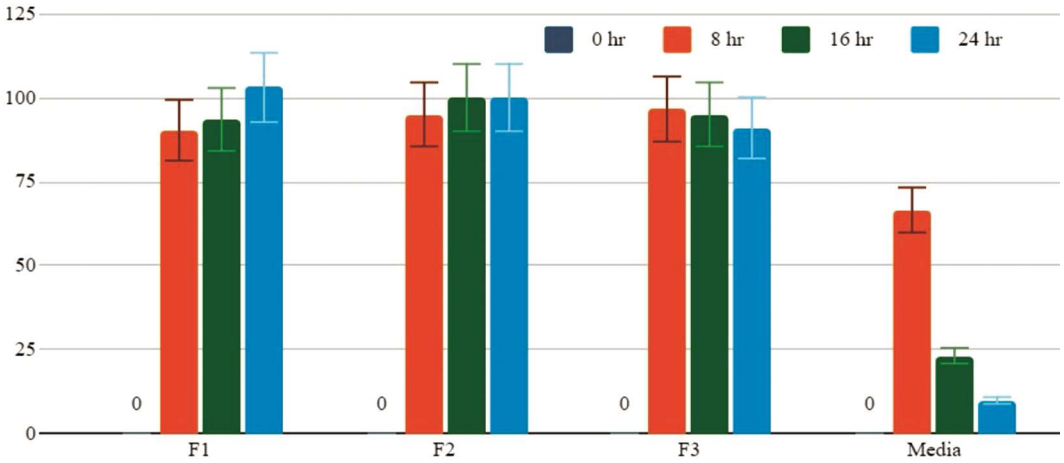

Fig. 10 — Percentage of wound healing over time for MRC-5 cells treated with different formulations [F1, F2 without glycerol, F3 with 30 mg/ml FA, and control (media only)] was measured at 0, 8, 16, and 24 h post-scratch (n = 3)

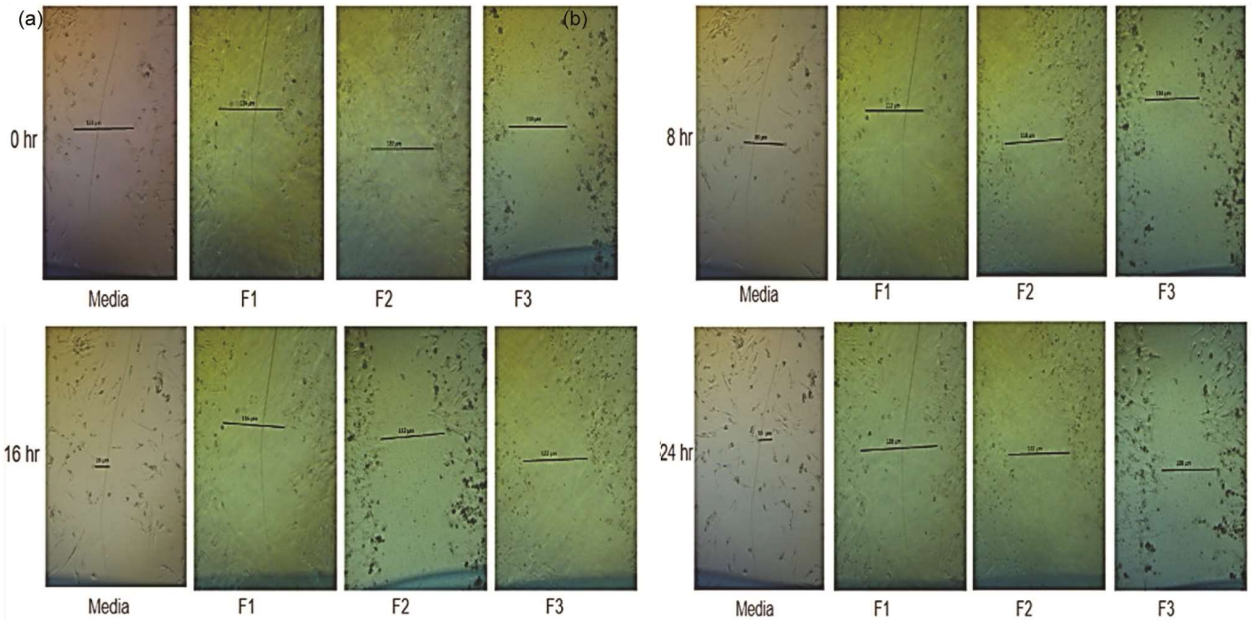

Fig. 11 — Representative images of the scratch assay results for MRC-5 cells treated with different formulations at 0 h, 8 h, 16 h, and 24 h

additive for antibacterial or antioxidant activity. The current hydrogel combines chitosan, chondroitin sulphate, ferulic acid, and κ-carrageenan, forming a multifunctional biomaterial to treat multiple stages of the wound healing process at once. Chitosan also offers antimicrobial activity and haemostasis, chondroitin sulphate mimics components of the extracellular matrix that aid fibroblast adhesion and tissue regeneration, ferulic acid provides strong antioxidant and anti-inflammatory effects to combat oxidative stress in chronic wounds, and κ-carrageenan enhances the mechanical stability and swelling of the hydrogel matrix to maintain moisture and manage exudates. The combined components offer a wider therapeutic functionality compared to previously reported chitosan-based hydrogels containing a single bioactive agent. The *in vitro* results indicate the wound healing potential of the hydrogel, but further studies in diabetic wound models are necessary to validate the therapeutic efficacy of this hydrogel under chronic wound conditions.

Conclusion

In this study, chitosan-based hydrogels enriched with chondroitin sulphate and ferulic acid were successfully developed and comprehensively characterized, demonstrating optimal fabrication with consistent thickness and favourable properties such as appropriate swelling ratios, mechanical characteristics closely matching human skin, and excellent moisture retention capabilities necessary for effective wound management, and confirmed by FTIR spectroscopy of the successful integration and interactions among the components, increasing structural integrity and bioactivity. Drug release profiles from controlled release studies showed sustained drug release profiles for long-term therapeutic effects, and antibacterial evaluations confirmed the possibility of decreasing infection at the wound site. In addition, molecular docking studies offered an understanding of the therapeutic mechanisms and suggested that structural modifications could further improve pharmacological performance. Moreover, results of scratch assay showed that all formulations (F1, F2, and F3) promote cell migration and accelerate wound closure *in vitro*. Collectively, these findings indicate that these bioactive chitosan-based hydrogels could be developed as potential advanced wound dressings.

Acknowledgement

This work was supported by Research Excellence and Innovation Grant (Project Code: REIG-FPS-2025/033) under the Centre of Excellence in Research, Value Innovation and Entrepreneurship (CERVIE), UCSI University, Malaysia.

Conflict of interest

All authors declare no conflict of interest.

References

1 Lopez-Ojeda W, Pandey A, Alhajj M & Oakley AM, Anatomy, skin (integument). *StatPearls*, (2022) 14.

2 Jiao Q, Zhi L, You B, Wang G, Wu N & Jia Y, Skin homeostasis: mechanism and influencing factors. *J Cosmet Dermatol*, 23 (2024) 1518.

3 Wernick B, Nahirniak P & Stawicki SP, Impaired wound healing. *StatPearls*, (2023) 67.

4 Burgess JL, Wyant WA, Abdo Abujamra B, Kirsner RS & Jozic I, Diabetic wound-healing science. *Medicina (B Aires)*, 57 (2021) 1072.

5 Pereira M, Vilaça M, Pedras S, Carvalho A, Vedhara K, Dantas M & Machado L, Wound healing and healing process in patients with diabetic foot ulcers: a survival analysis study. *Diabetes Res Clin Pract*, 198 (2023) 110623.

6 Sen CK, Human wound and its burden: Updated 2022 compendium of estimates. *Adv Wound Care (New Rochelle)*, 12 (2023) 657.

7 Nuutila K & Eriksson E, Moist wound healing with commonly available dressings. *Adv Wound Care (New Rochelle)*, 10 (2021) 685.

8 Moradifar F, Sepahdoost N, Tavakoli P & Mirzapoor A, Multi-functional dressings for recovery and screenable treatment of wounds: a review. *Heliyon*, 11 (2025) 41465.

9 Zheng Y, Pan C, Xu P & Liu K, Hydrogel-mediated extracellular vesicles for enhanced wound healing: the latest progress, and their prospects for 3D bioprinting. *J Nanobiotechnol*, 22 (2024) 57.

10 Zhang W, Liu L, Cheng H, Zhu J, Li X, Ye S & Li X, Hydrogel-based dressings designed to facilitate wound healing. *Mater Adv*, 5 (2024) 1364.

11 Zhang MX, Zhao WY, Fang QQ, Wang XF, Chen CY, Shi BH, Zheng B, Wang SJ, Tan WQ & Wu LH, Effects of chitosan-collagen dressing on wound healing *in vitro* and *in vivo* assays. *J Appl Biomater Funct Mater*, 9 (2021) 9698.

12 Hodaei H, Esmaeili Z, Erfani Y, Esnaashari SS, Geravand M & Adabi M, Preparation of biocompatible Zein/Gelatin/ Chitosan/PVA-based nanofibers loaded with vitamin E-TPGS *via* dual-opposite electrospinning method. *Sci Rep*, 14 (2024) 23796.

13 Guo Y, Yuan T, Xiao Z, Tang P, Xiao Y, Fan Y & Zhang X, Hydrogels of collagen/chondroitin sulfate/hyaluronan interpenetrating polymer network for cartilage tissue engineering. *J Mater Sci Mater Med*, 23 (2012) 2267.

14 Freedman BR, Hwang C, Talbot S, Hibler B, Matoori S & Mooney DJ, Breakthrough treatments for accelerated wound healing. *Sci Adv*, 9 (2023) 7007.

15 Purushothaman JR & Rizwanullah Md, Ferulic acid: a comprehensive review. *Cureus*.

16 Lin Y, Miao L, Li X, Qian L, Mu Q, Liu B, Ge X & Leng X, Effects of ferulic acid on the growth performance, physiological and biochemical functions, and hepato-intestinal health of blunt snout bream, *Megalobrama amblycephala*. *Aquac Rep*, 33 (2023) 101879.

17 Polaka S, Katare P, Pawar B, Vasdev N, Gupta T, Rajpoot K, Sengupta P & Tekade RK, Emerging ROS-modulating technologies for augmentation of the wound healing process. *ACS Omega*, 7 (2022) 30657.

18 Chopra H, Bibi S, Kumar S, Khan MS, Kumar P, Singh I. Preparation and evaluation of chitosan/PVA-based hydrogel films loaded with honey for wound healing application. *Gels*, 8 (2022) 111.

19 Tolstova T, Drozdova M, Popyrina T, Matveeva D, Demina T, Akopova T, Andreeva E & Markvicheva E, Preparation and *in vitro* evaluation of chitosan-g-oligolactide-based films and macroporous hydrogels for tissue engineering. *Polymers (Basel)*, 15 (2023) 907.

20 Evmenenko G, Alexeev V, Budtova T, Buyanov A & Frenkel S, Swelling-induced structure changes of polyelectrolyte gels. *Polymer (Guildf)*, 40 (1999) 2975.

21 Timur M & Paşa A, Synthesis, characterization, swelling, and metal uptake studies of aryl cross-linked chitosan hydrogels. *ACS Omega*, 3 (2018) 17416.

22 Chopra H, Bibi S, Kumar S, Khan MS, Kumar P & Singh I, Preparation and evaluation of chitosan/PVA-based hydrogel films loaded with honey for wound healing application. *Gels*, 8 (2022) 111.

23 Alven S & Aderibigbe BA, Chitosan and cellulose-based hydrogels for wound management. *Int J Mol Sci*, 21 (2020) 1.

24 Kumar PV, Abdelkarim Maki MA, Takahje ML, Wei YS, Tatt LM & Bin Abdul Majeed AB, Detection of formation of recombinant human keratinocyte growth factor-loaded chitosan nanoparticles based on its optical properties. *Curr Nanosci*, 14 (2018) 127.

25 Gull N, Khan SM, Zahid Butt MT, Khalid S, Shafiq M, Islam A, Asim S, Hafeez S & Khan RU, *In vitro* study of chitosan-based multi-responsive hydrogels as drug release vehicles: a preclinical study. *RSC Adv*, 9 (2019) 31078.

26 Korsmeyer RW, Gurny R, Doelker E, Buri P & Peppas NA, Mechanisms of solute release from porous hydrophilic polymers. *Int J Pharm*, 15 (1983) 25.

27 Higuchi T, Mechanism of sustained-action medication. Theoretical analysis of rate of release of solid drugs dispersed in solid matrices. *J Pharm Sci*, 52 (1963) 1145.

28 Costa P & Sousa Lobo JM, Modeling and comparison of dissolution profiles. *Eur J Pharm Sci*, 13 (2001) 123.

29 Farasati Far B, Naimi-Jamal MR, Jahanbakhshi M, Hadizadeh A, Dehghan S & Hadizadeh S, Enhanced antibacterial activity of porous chitosan-based hydrogels crosslinked with gelatin and metal ions. *Sci Rep*, 14 (2024) 7505.

30 Maki MAA, Teng MS, Tan KF & Kumar PV, Polyamidoamine-stabilized and hyaluronic acid-functionalized gold nanoparticles for cancer therapy. *OpenNano*, 13 (2023) 100182.

31 Tee YN, Kumar PV, Maki MAA, Elumalai M, Rahman SAKMEH & Cheah SC, Mucoadhesive low molecular chitosan complexes to protect rHuKGF from proteolysis: *in vitro* characterization and FHs 74 Int cell proliferation studies. *Curr Pharm Biotechnol*, 22 (2021) 969.

32 Liang CC, Park AY & Guan JL, *In vitro* scratch assay: a convenient and inexpensive method for analysis of cell migration *in vitro*. *Nat Protoc*, 2 (2007) 329.

33 Chong KJ, Feng H, Letchumanan V, Arip M, Fatokun O, Mochamad L, Ng CT, Chinnapan S & Selvaraja M, Tackling Microbial Resistance and Emerging Pathogens with Next-Generation Antibiotics. *Prog Microbes Mol Biol*, 7 (2024) 1.

34 Alabdali AYM, Khalid R, Kzar M, Ezzat MO, Huei GM, Hsia TW, Mogana R, Rahman H, Razik BMA, Issac PK, Chinnappan S & Khalivulla SI, Design, synthesis, *in silico* and antibacterial evaluation of curcumin derivatives loaded nanofiber as potential wound healing agents. *J King Saud Univ Sci*, 34 (2022) 102205.

35 Khanna K, Sharma N, Karwasra R, Kumar A, Nishad DK, Janakiraman AK, Ram Mani R, Rajagopal M, Tayyab S & Goel B, Exploring nalbuphine loaded chitosan nanoparticles for effective pain management through intranasal administration: a comparative study. *J Drug Target*, 33 (2025) 99.

36 Zolkiffly SZI, Hazizul Hasan M, Jusoh SA, Janakiraman AK, Sukumaran SK, Husain N, Zakaria Y & Jayasingh Chellammal HS, *In silico* and *in vivo* evaluations of fisetin and fisetin-loaded nanosuspension on monoamine oxidase inhibition in Aβ(25–35) induced dementia in mice model. *Pharmacol Res - Mod Chin Med*, 13 (2024) 100547.

37 Bülbül EÖ, Okur ME, Okur NÜ & Siafaka PI, Traditional and advanced wound dressings: physical characterization and desirable properties for wound healing. In *Nat Polym Wound Heal Repair* (Elsevier), (2022) 19.

38 Du J, Zhang Y, Huang Y, Zhang Q, Wang W, Yu M, Xu L & Xu J, Dual-Cross-Linked Chitosan-Based Antibacterial Hydrogels with Tough and Adhesive Properties for Wound Dressing. *Macromol Rapid Commun*, 44 (2023) 2300325.

39 Gómez MA, Bonilla JM, Coronel MA, Martínez J, Morán-Trujillo L, Orellana SL, Vidal A, Giacaman A, Morales C, Torres-Gallegos C & Concha M, Antibacterial activity against *Staphylococcus aureus* of chitosan/ chondroitin sulfate nanocomplex aerogels alone and enriched with erythromycin and elephant garlic (*Allium ampeloprasum* L. var. ampeloprasum) extract. *Pure Appl Chem*, 25 (2018) 885.